Optical transmission in highly concentrated dispersions

Rajeev Garg, Robert K. Prud'homme, and Ilhan A. Aksay

Department of Chemical Engineering and Princeton Materials Institute, Princeton University, Princeton, New Jersey 08544

Feng Liu and Robert R. Alfano

Institute for Ultrafast Spectroscopy and Lasers, Departments of Physics and Electrical Engineering and New York State Center of Advanced Technology for Ultrafast Photonic Materials and Applications, The City College and the Graduate Center of the City University of New York, New York, New York 10031

Received June 10, 1997; revised manuscript received September 11, 1997; accepted October 6, 1997

The intensity temporal profiles of diffusive light propagation in highly concentrated (up to volume fraction $\phi \sim 0.55$) dispersions measured by 100-fs laser pulses showed an increase in transport scattering mean free path above a critical concentration. This observation confirms the previous theoretical predictions of enhanced transmission at high particle concentrations due to correlated scattering. The correlation effects are accounted for by incorporating a hard sphere Percus–Yevick static structure factor into the prediction of transport mean free path. © 1998 Optical Society of America [S0740-3232(98)00803-5]

OCIS codes: 290.1990, 290.4210, 260.2030.

1. INTRODUCTION

The study of light scattering in concentrated systems has a history that goes back to the classic papers by Twersky and co-workers,[1,2] who attributed the transparency of the cornea to correlated scattering effects at high concentrations of collagen fibers. Twersky's[2] explanation invokes intercollagen fiber spatial separations that are small relative to the wavelength of light and leads to the conclusion that the transmitted light intensity should decrease with collagen concentration in uncorrelated dilute systems and increase with concentration in highly concentrated systems. Ishimaru and Kuga[3] were the first to partially demonstrate this phenomenon with 91-nm latex particles where isotropic scattering from individual scatterers was assumed since the scatterers were much smaller than the wavelength of light. However, Ishimaru and Kuga could not work with particle sizes close to the wavelength of light, owing to difficulties in measuring attenuation constants at high densities.

In applications where the scattering objects are comparable in size to the wavelength of light and the refractive-index contrast is large, a quantitative description of the scattering must include both particle correlations and the angular dependence of the scattered light. Our interest in such systems arises from stereolithography,[4] a new technique for rapid prototyping of ceramic objects with highly concentrated dispersions. In this application, a laser beam is focused onto a highly scattering ceramic dispersion to induce photocuring of an agent in the continuous liquid phase. A quantitative model of light propagation in the ceramic dispersion is needed to predict curing depths; to calculate lateral light dispersion, which will cause broadening of cured lines; and to determine the spatial profile of photon intensity to program laser-writing beam speeds required for curing. Similarly, medical applications of imaging through highly scattering tissue require a quantitative description of light scattering in highly concentrated dispersions.[5]

The framework for this quantitative description has been provided by several researchers,[6,7] who formulated the problem for light attenuation through colloidal dispersions using the diffusion model of the transport theory of light propagation.[8,9] The diffusion model is now well established for describing light propagation in highly scattering and absorbing media. The important parameter in the model is the transport mean free path of light. Beard *et al.*[1] and Twersky[2] showed that for isotropic scatterers the transport length in a correlated multiple-scattering medium is modified by the structure factor. For anisotropic scattering the generalization is straightforward.[9] Individual scattering is described by Mie scattering theory, and correlations are incorporated through the structure factor, $S(q)$, which is known for hard-sphere mixtures. The theory predicts that in the dilute limit the transport length should decrease linearly as the particle concentration increases. For correlated scatterers the decrease in transport length is less than linear. Interestingly, at high enough concentration, the transport length increases with particle concentration. Saulnier *et al.*[6] and Fraden and Maret[7] confirmed the deviations of the transport length (l_{tr}) from linearity in volume fraction. However, they did not experimentally study concentrations that were high enough to observe a decrease in scattering intensity with increase in volume fraction. Kaplan *et al.*[10] studied bimodal mixtures of latex spheres to 30 vol. %. Surprisingly, the addition of small spheres to a relatively dilute dispersion of large spheres resulted in a decrease in scattering intensity.

0740-3232/98/040932-04$15.00

This effect was attributed to the ordering that arises in the binary mixture.[11]

In this study we present what is the first, to our knowledge, demonstration of decreased scattering in highly concentrated (to 55 vol. %) dispersions of particles that are in the size range of the wavelength of light. Experiments were conducted with ultrashort-pulsed-laser spectroscopy and picosecond time-resolved detection to measure the temporal photon-transmission profiles. This is a far more rigorous test of the adequacy of the transport theory to describe photon propagation than is measurement of steady-state light transmission, which is an integral measure. We find that the transport theory best describes temporal light propagation over the entire range of concentrations with no adjustable parameters when Mie scattering is used to describe single-particle scattering and the Percus–Yevick (PY) theory is used to describe particle correlations.

2. THEORY

The diffuse light intensity in a medium is given by the diffusion equation[12]

$$\left[\frac{\partial}{\partial t} - D\nabla^2 + \frac{c}{l_a}\right] I(\mathbf{r}, t) = f(\mathbf{r}, t), \tag{1}$$

where $f(\mathbf{r}, t)$ represents the source function for the diffusing photons and the diffusion coefficient D is defined by $D = cl_{tr}/3$, where c is the speed of light in the medium and l_a is the absorption length in the medium. In this study, a narrow beam of ultrashort laser pulses was incident normally onto a scattering slab. The transmitted pulses at the point on the opposite side of the slab were measured. The transmitted pulse can be described by the solution of diffusion Eq. (1) for the slab geometry. The solution is given by[13]

$$I_z(t) = \frac{1}{4d^2t} \sum_{m=1}^{\infty} m \sin(m\pi z/d) \times \exp[-Dt(m\pi/d)^2]\exp(-ct/l_a), \tag{2}$$

where $d = z + 2z_0$, $z_0 = 0.71l_{tr}$ is the extrapolation length, and z is the thickness of the slab. In obtaining the above solution, perfectly absorbing boundary conditions at the extrapolated surfaces are used. Equation (2) was used to fit the experimental transmitted pulse profiles to determine the absorption and transport length of the medium. In fitting, the velocity of light in the medium was assumed to be the same as the velocity in water.

The transport mean free path is given by $l_{tr} = (n\sigma_{tr})^{-1}$, where σ_{tr} is the transport scattering cross section of a single scatterer and n is the number density of scatterer, which is related to the volume fraction ϕ by $n = \phi/v_p$, and v_p is the volume of a single scatterer. σ_{tr} for a nonabsorbing particle is given by

$$\sigma_{tr} = \int \frac{d\sigma}{d\Omega}[1 - \cos(\theta)]S(\theta)d\Omega, \tag{3}$$

where $d\sigma/d\Omega$ is the differential scattering cross section, which is reduced by a factor of $[1 - \cos(\theta)]$ owing to anisotropic scattering. Physically this means that for an anisotropic scatterer, more scattering events will be required to randomize the direction of light propagation in comparison with the isotropic case.[9] The interparticle structure factor $S(q)$ to account for particle correlations is

$$S(q) = 1 + n\int [g(r) - 1]\exp(i\mathbf{q}r)d^3\mathbf{r}, \tag{4}$$

where $g(r)$ is the radial distribution function and $\mathbf{q}$ is the scattering vector of the scattered photon and is related to the scattering angle by $\mathbf{q} = 2\mathbf{k}\sin(\theta/2)$. At high particle concentrations, dependent scattering takes place[14]; i.e., the interaction of radiation with a particle is affected by the presence of other particles in its vicinity. In dependent scattering, not only are the photons scattered from one particle rescattered by other particles, but also there is far-field interference of the scattered waves from different particles. The structure factor $S(\mathbf{q})$ in Eq. (4) describes the interplay among the scattering waves from different scatterers. For the case of hard spheres the PY structure factor[15] can be analytically obtained, and it is used in the present work.

3. EXPERIMENTS

A. Materials

The alumina dispersions were prepared by adding the powder (0.32 and 0.51 μm diameter, Sumitomo Chemical, refractive index 1.77) to water, with use of a 15,000-Mw ammonium salt of poly methacrylic acid (R. T. Vanderbilt Company, Inc.) as the dispersant. The dispersions were then ultrasonicated for a few minutes to homogenize. The samples at various volume fractions were prepared by dilution. The silica dispersions (0.46 μm diameter, Nissan Chemicals, refractive index 1.49) were purified by centrifugation to obtain a dispersion of monodisperse particles. The dispersions at different concentrations were then prepared by dilution.

B. Setup

The experimental system used to measure the intensity temporal profiles of transmitted light pulses is schematically shown in Fig. 1. Ultrashort laser pulses of 100 fs

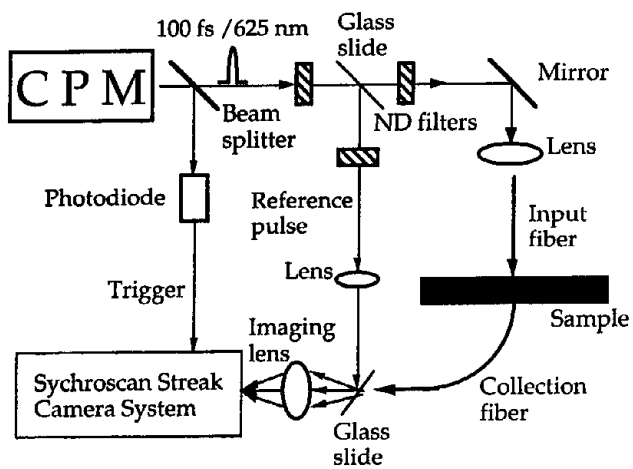

Fig. 1. Schematic diagram of experimental apparatus.

duration at a wavelength of 625 nm and 82 MHz repetition rate were generated by a colliding-pulse mode-locked laser. Part of the laser beam was split by a glass slide to be used as a reference pulse that marks the zero time of the signal beam and monitors the intensity of laser pulses. The main part of the beam was coupled into an optical fiber (core diameter 200 μm) that was positioned near the front face of the sample cell. The sample cell consisted of two glass windows (50 mm × 50 mm) with 1- to 5-mm spacers. The sample thickness was much larger than l_{tr}, so the diffusion approximation is valid. The transmitted light was collected by another optical fiber (core diameter 200 μm) and was imaged into a streak-camera detection system (10 ps time resolution). The scattered light was time resolved by the streak camera and recorded on a CCD camera. Neutral density filters were used to adjust the incident light level for intensity comparison among scattered-pulse profiles obtained from different samples.

4. RESULTS

Figure 2 shows the transmitted temporal profiles for dispersions of 0.51-μm alumina particles. As the volume fraction increases from 0.1 to 0.55, the peak intensity of the transmitted pulses decreases and the pulses broaden since the transport length decreases as the particle concentration increases. Figure 3 shows the temporal profile for aqueous dispersions of 0.32-μm alumina particles at various volume fractions. The transmitted intensity decreases as ϕ increases from 0.02 to 0.3, but as ϕ is increased beyond 0.3 the transmitted intensity increases as ϕ increases (inset, Fig. 3). This reflects increasing l_{tr} with ϕ at higher ϕ. The 0.46-μm silica particles show similar behavior where an upturn in l_{tr} occurs at ϕ value of 0.47 (not shown).

In Fig. 4, the transport mean free path length for the alumina and silica dispersions as a function of volume fraction ϕ are plotted. The solid curve corresponds to l_{tr}

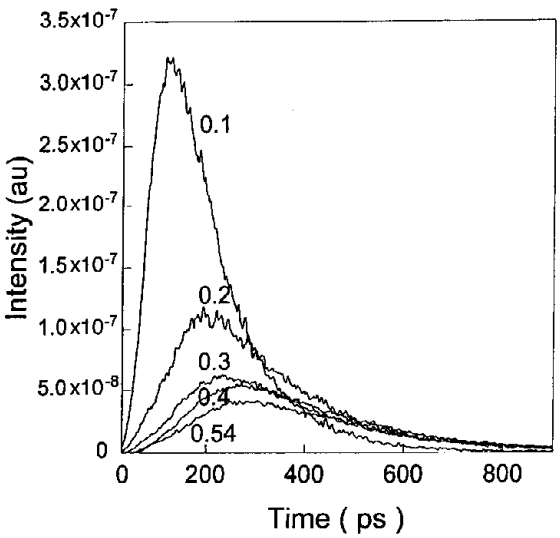

Fig. 2. Transmitted temporal profiles for aqueous dispersion of 0.51-μm alumina particles obtained in 2-mm-thick scattering samples at the ϕ values indicated. The intensity scale is normalized to the same incident intensity.

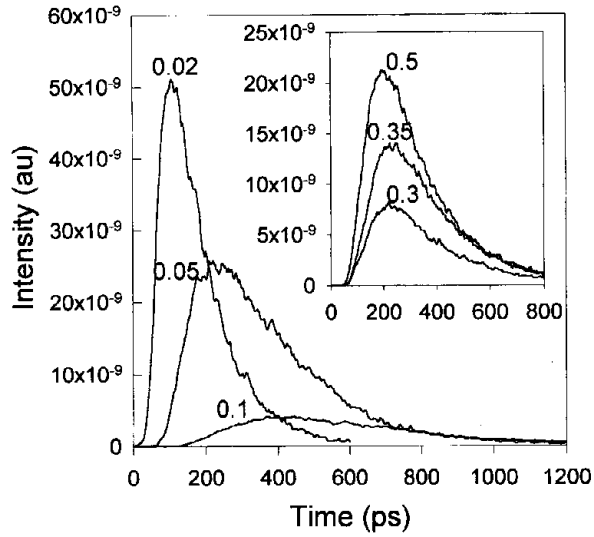

Fig. 3. Transmitted temporal profiles for aqueous dispersions of 0.32-μm alumina particles at the ϕ values indicated. The thickness of the scattering samples for ϕ values of 0.02, 0.05, and 0.1 was 2 mm and for 0.3, 0.35 and 0.5 was 1 mm.

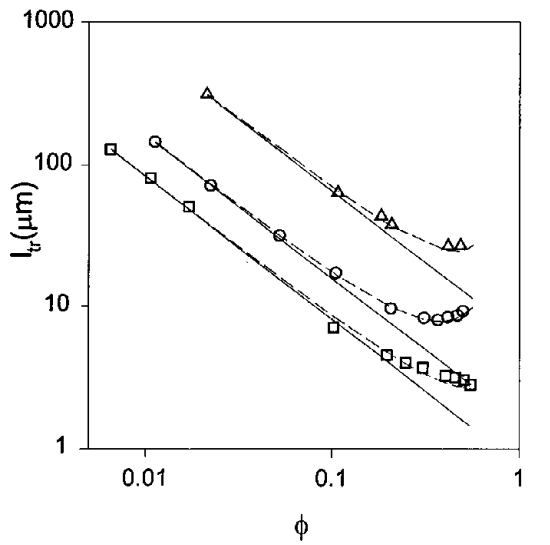

Fig. 4. Transport mean free path versus volume fraction of scattering particles on log–log scale. Solid curves are computed values without correlations and σ_{tr} from Mie theory; dashed curves, computed values obtained by using Eq. (3) and $S(\theta)$ from PY. Symbols represent transport lengths obtained from the experimental temporal profiles: squares, 0.51-μm alumina; circles, 0.32-μm alumina; triangles, 0.46-μm silica. The curve for 0.51-μm alumina has been shifted up by log (3) for clarity.

calculated without the correlation effects [$S(q) = 1$] and shows linearly decreasing l_{tr} with ϕ. The dashed curves are the l_{tr} calculated from Eq. (3) by using the hard-sphere PY structure factor to account for correlations and the Mie theory to calculate the differential scattering cross section.[16] The symbols are the experimentally obtained values from the fitting of Eq. (2) to the temporal profiles. In all the samples studied, the absorption length was 4–5 orders of magnitude larger than the transport length, because the particles are nonabsorbing. As can be seen, the experimental l_{tr} values are in good agreement with the theory when the correlation effects

are taken into account. At very high ϕ, the correlation effects become strong enough to cause an increase in the l_{tr} (in two of the systems, 0.32-μm alumina and 0.46-μm silica) with further increase of ϕ, as is predicted by the theory. The ϕ at which reversal in l_{tr} occurs is higher for larger particle size. The differences among these three systems are discussed below. To our knowledge this is the first experimental work that probes the concentrated dispersions at such high volume fractions, where the transport mean free path length increases with increasing particle concentration.

5. DISCUSSION

As shown in Fig. 4, the correlation effects can enhance l_{tr} by as much as a factor of 4 over that expected from the uncorrelated case. This is in agreement with earlier work,[7] where the l_{tr} was found to be doubled at the highest densities studied ($\phi \sim 0.2$). It was suggested that the correlation effects are important only when the number of scatterers per cubic wavelength ($n\lambda^3$) is greater than 1. We observe a large correlation effect even for $n\lambda^3 = 0.5$, where l_{tr} is doubled for 0.51-μm alumina particles. As the particle separation scales with $\phi^{-1/3}$, for the system studied it is estimated that interparticle separation will be comparable to λ for $\phi \sim 0.2$, which is where correlation effects begin to affect the scattering. This observation suggests that interparticle separation is the most critical parameter for the correlation effects, as was predicted by Lee.[14] As the interparticle spacing becomes comparable to or less than the wavelength of light, the correlation effects become significant.

The correlation effects are shown to be stronger for smaller particle size (compare the curves for 0.32- and 0.51-μm alumina particles). For example, at $\phi = 0.45$, l_{tr} is enhanced by a factor of 2.6 for 0.32-μm alumina particles over that of the uncorrelated case, whereas for 0.51-μm alumina particles the enhancement is 1.7. This is again due to the fact that interparticle spacing decreases faster for smaller particles with ϕ and thus causes stronger correlation effects. The correlation effects are similar for similar-size particles (compare the curves for 0.51-μm alumina and 0.46-μm silica particles in Fig. 4). For example at $\phi = 0.4$, l_{tr} is enhanced by a factor of 1.5 for 0.51-μm alumina particles over that of the uncorrelated case, and for 0.46-μm silica particles the enhancement is 1.6.

6. CONCLUSIONS

In conclusion, the diffusive transport theory adequately describes the phenomena of laser pulse propagation in highly concentrated, highly scattering colloidal dispersions. At a high volume fraction of particles, when the interparticle spacing becomes comparable to or less than the wavelength, the correlation effects significantly enhance l_{tr} over that of an uncorrelated case and at very high ϕ can even lead to an increase in l_{tr} with increasing ϕ. This was observed for 0.32-μm alumina and 0.46-μm silica particle dispersions as the transmitted intensity and l_{tr} first decreases as ϕ increases, goes through a minimum, and starts increasing as ϕ is further increased. The maximum in the transmitted temporal intensity profiles increases by a factor of 3 in going from $\phi = 0.3$ to $\phi = 0.5$ for the 0.32-μm alumina particles. The correlation effects can be adequately accounted for by modifying the transport cross section of the particle by the PY hard-sphere static-structure factor. For laser stereolithography this implies that the combination of decreased particle size and increased concentrations offers increased curing depths. The success of the model in representing the data means that design algorithms for stereolithography photocuring should be possible.

ACKNOWLEDGMENTS

This work was funded by the U.S. Army Research Office under Multidisciplinary University Research Initiative grant DAAH04-95-1-0102. Partial support for the work at The City College of New York was obtained from the New York State Science and Technology Foundation.

REFERENCES

1. C. I. Beard, T. H. Kays, and V. Twersky, "Scattering by random distribution of spheres vs. concentration," IEEE Trans. Antennas Propag. **AP-15**, 99–118 (1967).
2. V. Twersky, "Transparency of pair correlated, random distribution of small scatterers with applications to the cornea," J. Opt. Soc. Am. **65**, 524–530 (1975).
3. A. Ishimaru and Y. Kuga, "Attenuation constant of a coherent field in dense distribution of particles," J. Opt. Soc. Am. **72**, 1317–1320 (1982).
4. P. F. Jacobs, *Rapid Prototyping and Manufacturing—Fundamentals of Stereolithography* (Society of Manufacturing Engineers, Dearborn, Mich., 1992).
5. L. Feng, K. M. Yoo, and R. R. Alfano, "Ultrafast laser pulse transmission and imaging through biological tissues," Appl. Opt. **32**, 554–558 (1993).
6. P. M. Saulnier, M. P. Zinkin, and G. H. Watson, "Scatterer correlation effects on photon transport in dense random media," Phys. Rev. B **42**, 2621–2623 (1990).
7. M. Fraden and G. Maret, "Multiple scattering from concentrated, interacting suspensions," Phys. Rev. Lett. **65**, 512–515 (1990).
8. F. C. MacKintosh and J. Sajeev, "Diffusion wave spectroscopy and multiple scattering of light in correlated random media," Phys. Rev. B **40**, 2383–2406 (1989).
9. D. J. Pine, D. A. Weitz, G. Maret, P. E. Wolf, E. Herbolzheimer, and P. M. Chaikin, "Dynamical correlations of multiply scattered light," in *Scattering and Localization of Classical Waves in Random Media*, P. Sheng, ed. (World Scientific, Singapore, 1990), pp. 312–371.
10. P. D. Kaplan, A. G. Yodh, and D. J. Pine, "Diffusion and structure in dense binary suspensions," Phys. Rev. Lett. **68**, 393–396 (1992).
11. P. D. Kaplan, "Optical studies of the structure and dynamics of opaque colloids," Ph.D. dissertation (University of Pennsylvania, Philadelphia, Pa., 1993).
12. A. Ishimaru, *Wave Propagation and Scattering in Random Media*, Vols. 1 and 2, (Academic, New York, 1978), p. 175.
13. M. Lax, V. Narayanamurti, and R. C. Fulton, "Classical diffusive photon transport in a slab," in *Proceedings of the Symposium on Laser Optics and Condensed Matter, Leningrad, June 1987*, J. L. Birman and H. Z. Cumins, eds. (Plenum, New York, 1987), pp. 229–235.
14. S.-C. Lee, "Dependent scattering by parallel fibers: effects of multiple scattering and wave interferences," J. Thermophys. Heat Tr. **6**, 589–595 (1990).
15. N. W. Ashcroff and J. Lekner, "Structure and resistivity of liquid metals," Phys. Rev. **145**, 83–90 (1966).
16. C. F. Bohren and D. R. Huffman, *Absorption and Scattering of Light by Small Particles* (Wiley, New York, 1983), p. 126.